2012-11-9

Precision Measurement of the $B \to X_s \gamma$ Photon Energy Spectrum, Branching Fraction, and Direct CP Asymmetry $A_{CP}(B \to X_{s+d} \gamma)$

J. P. Lees, *et al.*

Precision Measurement of the $B \to X_s\gamma$ Photon Energy Spectrum, Branching Fraction, and Direct CP Asymmetry $A_{CP}(B \to X_{s+d}\gamma)$

J. P. Lees,[1] V. Poireau,[1] V. Tisserand,[1] J. Garra Tico,[2] E. Grauges,[2] A. Palano,[3a,3b] G. Eigen,[4] B. Stugu,[4] D. N. Brown,[5] L. T. Kerth,[5] Yu. G. Kolomensky,[5] G. Lynch,[5] H. Koch,[6] T. Schroeder,[6] D. J. Asgeirsson,[7] C. Hearty,[7] T. S. Mattison,[7] J. A. McKenna,[7] R. Y. So,[7] A. Khan,[8] V. E. Blinov,[9] A. R. Buzykaev,[9] V. P. Druzhinin,[9] V. B. Golubev,[9] E. A. Kravchenko,[9] A. P. Onuchin,[9] S. I. Serednyakov,[9] Yu. I. Skovpen,[9] E. P. Solodov,[9] K. Yu. Todyshev,[9] A. N. Yushkov,[9] M. Bondioli,[10] D. Kirkby,[10] A. J. Lankford,[10] M. Mandelkern,[10] H. Atmacan,[11] J. W. Gary,[11] F. Liu,[11] O. Long,[11] G. M. Vitug,[11] C. Campagnari,[12] T. M. Hong,[12] D. Kovalskyi,[12] J. D. Richman,[12] C. A. West,[12] A. M. Eisner,[13] J. Kroseberg,[13] W. S. Lockman,[13] A. J. Martinez,[13] B. A. Schumm,[13] A. Seiden,[13] L. Winstrom,[13] D. S. Chao,[14] C. H. Cheng,[14] B. Echenard,[14] K. T. Flood,[14] D. G. Hitlin,[14] P. Ongmongkolkul,[14] F. C. Porter,[14] A. Y. Rakitin,[14] R. Andreassen,[15] Z. Huard,[15] B. T. Meadows,[15] M. D. Sokoloff,[15] L. Sun,[15] P. C. Bloom,[16] W. T. Ford,[16] A. Gaz,[16] U. Nauenberg,[16] J. G. Smith,[16] S. R. Wagner,[16] R. Ayad,[17,†] W. H. Toki,[17] B. Spaan,[18] K. R. Schubert,[19] R. Schwierz,[19] D. Bernard,[20] M. Verderi,[20] P. J. Clark,[21] S. Playfer,[21] D. Bettoni,[22a] C. Bozzi,[22a] R. Calabrese,[22a,22b] G. Cibinetto,[22a,22b] E. Fioravanti,[22a,22b] I. Garzia,[22a,22b] E. Luppi,[22a,22b] M. Munerato,[22a,22b] L. Piemontese,[22a] V. Santoro,[22a] R. Baldini-Ferroli,[23] A. Calcaterra,[23] R. de Sangro,[23] G. Finocchiaro,[23] P. Patteri,[23] I. M. Peruzzi,[23,‡] M. Piccolo,[23] M. Rama,[23] A. Zallo,[23] R. Contri,[24a,24b] E. Guido,[24a,24b] M. Lo Vetere,[24a,24b] M. R. Monge,[24a,24b] S. Passaggio,[24a] C. Patrignani,[24a,24b] E. Robutti,[24a] B. Bhuyan,[25] V. Prasad,[25] C. L. Lee,[26] M. Morii,[26] A. J. Edwards,[27] A. Adametz,[28] U. Uwer,[28] H. M. Lacker,[29] T. Lueck,[29] P. D. Dauncey,[30] U. Mallik,[31] C. Chen,[32] J. Cochran,[32] W. T. Meyer,[32] S. Prell,[32] A. E. Rubin,[32] A. V. Gritsan,[33] Z. J. Guo,[33] N. Arnaud,[34] M. Davier,[34] D. Derkach,[34] G. Grosdidier,[34] F. Le Diberder,[34] A. M. Lutz,[34] B. Malaescu,[34] P. Roudeau,[34] M. H. Schune,[34] A. Stocchi,[34] G. Wormser,[34] D. J. Lange,[35] D. M. Wright,[35] C. A. Chavez,[36] J. P. Coleman,[36] J. R. Fry,[36] E. Gabathuler,[36] D. E. Hutchcroft,[36] D. J. Payne,[36] C. Touramanis,[36] A. J. Bevan,[37] F. Di Lodovico,[37] R. Sacco,[37] M. Sigamani,[37] G. Cowan,[38] D. N. Brown,[39] C. L. Davis,[39] A. G. Denig,[40] M. Fritsch,[40] W. Gradl,[40] K. Griessinger,[40] A. Hafner,[40] E. Prencipe,[40] R. J. Barlow,[41,§] G. Jackson,[41] G. D. Lafferty,[41] E. Behn,[42] R. Cenci,[42] B. Hamilton,[42] A. Jawahery,[42] D. A. Roberts,[42] C. Dallapiccola,[43] R. Cowan,[44] D. Dujmic,[44] G. Sciolla,[44] R. Cheaib,[45] D. Lindemann,[45] P. M. Patel,[45,*] S. H. Robertson,[45] P. Biassoni,[46a,46b] N. Neri,[46a] F. Palombo,[46a,46b] S. Stracka,[46a,46b] L. Cremaldi,[47] R. Godang,[47,‖] R. Kroeger,[47] P. Sonnek,[47] D. J. Summers,[47] X. Nguyen,[48] M. Simard,[48] P. Taras,[48] G. De Nardo,[49a,49b] D. Monorchio,[49a,49b] G. Onorato,[49a,49b] C. Sciacca,[49a,49b] M. Martinelli,[50] G. Raven,[50] C. P. Jessop,[51] K. Knoepfel,[51] J. M. LoSecco,[51] W. F. Wang,[51] K. Honscheid,[52] R. Kass,[52] J. Brau,[53] R. Frey,[53] M. Lu,[53] N. B. Sinev,[53] D. Strom,[53] E. Torrence,[53] E. Feltresi,[54a,54b] N. Gagliardi,[54a,54b] M. Margoni,[54a,54b] M. Morandin,[54a] M. Posocco,[54a] M. Rotondo,[54a] G. Simi,[54a] F. Simonetto,[54a,54b] R. Stroili,[54a,54b] S. Akar,[55] E. Ben-Haim,[55] M. Bomben,[55] G. R. Bonneaud,[55] H. Briand,[55] G. Calderini,[55] J. Chauveau,[55] O. Hamon,[55] Ph. Leruste,[55] G. Marchiori,[55] J. Ocariz,[55] S. Sitt,[55] M. Biasini,[56a,56b] E. Manoni,[56a,56b] S. Pacetti,[56a,56b] A. Rossi,[56a,56b] C. Angelini,[57a,57b] G. Batignani,[57a,57b] S. Bettarini,[57a,57b] M. Carpinelli,[57a,57b,¶] G. Casarosa,[57a,57b] A. Cervelli,[57a,57b] F. Forti,[57a,57b] M. A. Giorgi,[57a,57b] A. Lusiani,[57a,57c] B. Oberhof,[57a,57b] E. Paoloni,[57a,57b] A. Perez,[57a] G. Rizzo,[57a,57b] J. J. Walsh,[57a] D. Lopes Pegna,[58] J. Olsen,[58] A. J. S. Smith,[58] A. V. Telnov,[58] F. Anulli,[59a] R. Faccini,[59a,59b] F. Ferrarotto,[59a] F. Ferroni,[59a,59b] M. Gaspero,[59a,59b] L. Li Gioi,[59a] M. A. Mazzoni,[59a] G. Piredda,[59a] C. Bünger,[60] O. Grünberg,[60] T. Hartmann,[60] T. Leddig,[60] H. Schröder,[60,*] C. Voss,[60] R. Waldi,[60] T. Adye,[61] E. O. Olaiya,[61] F. F. Wilson,[61] S. Emery,[62] G. Hamel de Monchenault,[62] G. Vasseur,[62] Ch. Yèche,[62] D. Aston,[63] D. J. Bard,[63] R. Bartoldus,[63] P. Bechtle,[63] J. F. Benitez,[63] C. Cartaro,[63] M. R. Convery,[63] J. Dorfan,[63] G. P. Dubois-Felsmann,[63] W. Dunwoodie,[63] M. Ebert,[63] R. C. Field,[63] M. Franco Sevilla,[63] B. G. Fulsom,[63] A. M. Gabareen,[63] M. T. Graham,[63] P. Grenier,[63] C. Hast,[63] W. R. Innes,[63] M. H. Kelsey,[63] P. Kim,[63] M. L. Kocian,[63] D. W. G. S. Leith,[63] P. Lewis,[63] B. Lindquist,[63] S. Luitz,[63] V. Luth,[63] H. L. Lynch,[63] D. B. MacFarlane,[63] D. R. Muller,[63] H. Neal,[63] S. Nelson,[63] M. Perl,[63] T. Pulliam,[63] B. N. Ratcliff,[63] A. Roodman,[63] A. A. Salnikov,[63] R. H. Schindler,[63] A. Snyder,[63] D. Su,[63] M. K. Sullivan,[63] J. Va'vra,[63] A. P. Wagner,[63] W. J. Wisniewski,[63] M. Wittgen,[63] D. H. Wright,[63] H. W. Wulsin,[63] C. C. Young,[63] V. Ziegler,[63] W. Park,[64] M. V. Purohit,[64] R. M. White,[64] J. R. Wilson,[64] A. Randle-Conde,[65] S. J. Sekula,[65] M. Bellis,[66] P. R. Burchat,[66] T. S. Miyashita,[66] M. S. Alam,[67] J. A. Ernst,[67] R. Gorodeisky,[68] N. Guttman,[68] D. R. Peimer,[68] A. Soffer,[68] P. Lund,[69] S. M. Spanier,[69] J. L. Ritchie,[70] A. M. Ruland,[70] R. F. Schwitters,[70] B. C. Wray,[70] J. M. Izen,[71] X. C. Lou,[71] F. Bianchi,[72a,72b] D. Gamba,[72a,72b] S. Zambito,[72a,72b] L. Lanceri,[73a,73b] L. Vitale,[73a,73b] F. Martinez-Vidal,[74] A. Oyanguren,[74] H. Ahmed,[75] J. Albert,[75] Sw. Banerjee,[75] F. U. Bernlochner,[75] H. H. F. Choi,[75] G. J. King,[75]

R. Kowalewski,[75] M. J. Lewczuk,[75] I. M. Nugent,[75] J. M. Roney,[75] R. J. Sobie,[75] N. Tasneem,[75] T. J. Gershon,[76] P. F. Harrison,[76] T. E. Latham,[76] E. M. T. Puccio,[76] H. R. Band,[77] S. Dasu,[77] Y. Pan,[77] R. Prepost,[77] and S. L. Wu[77]

(*BABAR* Collaboration)

[1]*Laboratoire d'Annecy-le-Vieux de Physique des Particules (LAPP), Université de Savoie, CNRS/IN2P3, F-74941 Annecy-Le-Vieux, France*
[2]*Universitat de Barcelona, Facultat de Fisica, Departament ECM, E-08028 Barcelona, Spain*
[3a]*INFN Sezione di Bari, I-70126 Bari, Italy*
[3b]*Dipartimento di Fisica, Università di Bari, I-70126 Bari, Italy*
[4]*University of Bergen, Institute of Physics, N-5007 Bergen, Norway*
[5]*Lawrence Berkeley National Laboratory and University of California, Berkeley, California 94720, USA*
[6]*Ruhr Universität Bochum, Institut für Experimentalphysik 1, D-44780 Bochum, Germany*
[7]*University of British Columbia, Vancouver, British Columbia, Canada V6T 1Z1*
[8]*Brunel University, Uxbridge, Middlesex UB8 3PH, United Kingdom*
[9]*Budker Institute of Nuclear Physics, Novosibirsk 630090, Russia*
[10]*University of California at Irvine, Irvine, California 92697, USA*
[11]*University of California at Riverside, Riverside, California 92521, USA*
[12]*University of California at Santa Barbara, Santa Barbara, California 93106, USA*
[13]*University of California at Santa Cruz, Institute for Particle Physics, Santa Cruz, California 95064, USA*
[14]*California Institute of Technology, Pasadena, California 91125, USA*
[15]*University of Cincinnati, Cincinnati, Ohio 45221, USA*
[16]*University of Colorado, Boulder, Colorado 80309, USA*
[17]*Colorado State University, Fort Collins, Colorado 80523, USA*
[18]*Technische Universität Dortmund, Fakultät Physik, D-44221 Dortmund, Germany*
[19]*Technische Universität Dresden, Institut für Kern- und Teilchenphysik, D-01062 Dresden, Germany*
[20]*Laboratoire Leprince-Ringuet, Ecole Polytechnique, CNRS/IN2P3, F-91128 Palaiseau, France*
[21]*University of Edinburgh, Edinburgh EH9 3JZ, United Kingdom*
[22a]*INFN Sezione di Ferrara, I-44100 Ferrara, Italy*
[22b]*Dipartimento di Fisica, Università di Ferrara, I-44100 Ferrara, Italy*
[23]*INFN Laboratori Nazionali di Frascati, I-00044 Frascati, Italy*
[24a]*INFN Sezione di Genova, I-16146 Genova, Italy*
[24b]*Dipartimento di Fisica, Università di Genova, I-16146 Genova, Italy*
[25]*Indian Institute of Technology Guwahati, Guwahati, Assam, 781 039, India*
[26]*Harvard University, Cambridge, Massachusetts 02138, USA*
[27]*Harvey Mudd College, Claremont, California 91711, USA*
[28]*Universität Heidelberg, Physikalisches Institut, Philosophenweg 12, D-69120 Heidelberg, Germany*
[29]*Humboldt-Universität zu Berlin, Institut für Physik, Newtonstr. 15, D-12489 Berlin, Germany*
[30]*Imperial College London, London, SW7 2AZ, United Kingdom*
[31]*University of Iowa, Iowa City, Iowa 52242, USA*
[32]*Iowa State University, Ames, Iowa 50011-3160, USA*
[33]*Johns Hopkins University, Baltimore, Maryland 21218, USA*
[34]*Laboratoire de l'Accélérateur Linéaire, IN2P3/CNRS et Université Paris-Sud 11, Centre Scientifique d'Orsay, B. P. 34, F-91898 Orsay Cedex, France*
[35]*Lawrence Livermore National Laboratory, Livermore, California 94550, USA*
[36]*University of Liverpool, Liverpool L69 7ZE, United Kingdom*
[37]*Queen Mary, University of London, London, E1 4NS, United Kingdom*
[38]*University of London, Royal Holloway and Bedford New College, Egham, Surrey TW20 0EX, United Kingdom*
[39]*University of Louisville, Louisville, Kentucky 40292, USA*
[40]*Johannes Gutenberg-Universität Mainz, Institut für Kernphysik, D-55099 Mainz, Germany*
[41]*University of Manchester, Manchester M13 9PL, United Kingdom*
[42]*University of Maryland, College Park, Maryland 20742, USA*
[43]*University of Massachusetts, Amherst, Massachusetts 01003, USA*
[44]*Massachusetts Institute of Technology, Laboratory for Nuclear Science, Cambridge, Massachusetts 02139, USA*
[45]*McGill University, Montréal, Québec, Canada H3A 2T8*
[46a]*INFN Sezione di Milano, I-20133 Milano, Italy*
[46b]*Dipartimento di Fisica, Università di Milano, I-20133 Milano, Italy*
[47]*University of Mississippi, University, Mississippi 38677, USA*
[48]*Université de Montréal, Physique des Particules, Montréal, Québec, Canada H3C 3J7*
[49a]*INFN Sezione di Napoli, I-80126 Napoli, Italy*

[49b]Dipartimento di Scienze Fisiche, Università di Napoli Federico II, I-80126 Napoli, Italy
[50]NIKHEF, National Institute for Nuclear Physics and High Energy Physics, NL-1009 DB Amsterdam, The Netherlands
[51]University of Notre Dame, Notre Dame, Indiana 46556, USA
[52]Ohio State University, Columbus, Ohio 43210, USA
[53]University of Oregon, Eugene, Oregon 97403, USA
[54a]INFN Sezione di Padova, I-35131 Padova, Italy
[54b]Dipartimento di Fisica, Università di Padova, I-35131 Padova, Italy
[55]Laboratoire de Physique Nucléaire et de Hautes Energies, IN2P3/CNRS, Université Pierre et Marie Curie-Paris6, Université Denis Diderot-Paris7, F-75252 Paris, France
[556a]INFN Sezione di Perugia, I-06100 Perugia, Italy
[56b]Dipartimento di Fisica, Università di Perugia, I-06100 Perugia, Italy
[57a]INFN Sezione di Pisa, I-56127 Pisa, Italy
[57b]Dipartimento di Fisica, Università di Pisa, I-56127 Pisa, Italy
[57c]Scuola Normale Superiore di Pisa, I-56127 Pisa, Italy
[58]Princeton University, Princeton, New Jersey 08544, USA
[59a]INFN Sezione di Roma, I-00185 Roma, Italy
[59b]Dipartimento di Fisica, Università di Roma La Sapienza, I-00185 Roma, Italy
[60]Universität Rostock, D-18051 Rostock, Germany
[61]Rutherford Appleton Laboratory, Chilton, Didcot, Oxon, OX11 0QX, United Kingdom
[62]CEA, Irfu, SPP, Centre de Saclay, F-91191 Gif-sur-Yvette, France
[63]SLAC National Accelerator Laboratory, Stanford, California 94309 USA
[64]University of South Carolina, Columbia, South Carolina 29208, USA
[65]Southern Methodist University, Dallas, Texas 75275, USA
[66]Stanford University, Stanford, California 94305-4060, USA
[67]State University of New York, Albany, New York 12222, USA
[68]Tel Aviv University, School of Physics and Astronomy, Tel Aviv, 69978, Israel
[69]University of Tennessee, Knoxville, Tennessee 37996, USA
[70]University of Texas at Austin, Austin, Texas 78712, USA
[71]University of Texas at Dallas, Richardson, Texas 75083, USA
[72a]INFN Sezione di Torino, I-10125 Torino, Italy
[72b]Dipartimento di Fisica Sperimentale, Università di Torino, I-10125 Torino, Italy
[73a]INFN Sezione di Trieste, I-34127 Trieste, Italy
[73b]Dipartimento di Fisica, Università di Trieste, I-34127 Trieste, Italy
[74]IFIC, Universitat de Valencia-CSIC, E-46071 Valencia, Spain
[75]University of Victoria, Victoria, British Columbia, Canada V8W 3P6
[76]Department of Physics, University of Warwick, Coventry CV4 7AL, United Kingdom
[77]University of Wisconsin, Madison, Wisconsin 53706, USA

(Received 12 July 2012; published 9 November 2012)

The photon spectrum in the inclusive electromagnetic radiative decays of the B meson, $B \to X_s\gamma$ plus $B \to X_d\gamma$, is studied using a data sample of $(382.8 \pm 4.2) \times 10^6 \Upsilon(4S) \to B\bar{B}$ decays collected by the *BABAR* experiment at SLAC. The spectrum is used to extract the branching fraction $\mathcal{B}(B \to X_s\gamma) = (3.21 \pm 0.33) \times 10^{-4}$ for $E_\gamma > 1.8$ GeV and the direct CP asymmetry $A_{CP}(B \to X_{s+d}\gamma) = 0.057 \pm 0.063$. The effects of detector resolution and Doppler smearing are unfolded to measure the photon energy spectrum in the B meson rest frame.

DOI: 10.1103/PhysRevLett.109.191801 PACS numbers: 13.20.He, 11.30.Er, 12.15.Hh

In the standard model (SM), the electromagnetic radiative decays of the b quark, $b \to s\gamma$ and $b \to d\gamma$, proceed via a loop diagram at leading order. A wide variety of new physics (NP) scenarios such as supersymmetry may cause new contributions to the loop [1–8] at the same order as the SM, resulting in significant deviations for both the branching fractions and the direct CP asymmetry

$$A_{CP} = \frac{\Gamma[b \to (s+d)\gamma] - \Gamma[\bar{b} \to (\bar{s}+\bar{d})\gamma]}{\Gamma[b \to (s+d)\gamma] + \Gamma[\bar{b} \to (\bar{s}+\bar{d})\gamma]}.$$

Inclusive hadronic branching fractions (BF) $\mathcal{B}(B \to X_s\gamma)$ and $\mathcal{B}(B \to X_d\gamma)$ can be equated with the perturbatively calculable partonic BF $\mathcal{B}(b \to s\gamma)$ and $\mathcal{B}(b \to d\gamma)$ at the level of a few percent [9], allowing theoretically clean predictions. At next-to-next-to-leading-order (four-loop), the SM calculation gives $\mathcal{B}(B \to X_s\gamma) = (3.15 \pm 0.23) \times 10^{-4}$ ($E_\gamma > 1.6$ GeV) [10], where E_γ is the photon energy measured in the rest frame of the B meson. $\mathcal{B}(B \to X_d\gamma)$ is suppressed by a factor of $|V_{td}/V_{ts}|^2 \approx 0.04$, where V_{ij} are the elements of the Cabbibo-Kobayashi-Mashawa (CKM) quark-mixing

matrix. NP with nonminimal flavor violation can also significantly enhance A_{CP} [11], which is approximately 10^{-6} in the SM [12–14]. Consequently the precision measurement of these decays has long been identified as important in the search for NP. They are central to the program of the future Super B factories [15–17], which will probe NP mass scales up to 100 TeV.

In this letter, new precise measurements of $\mathcal{B}(B \to X_s\gamma)$ and A_{CP} are presented. The analysis has been significantly improved from our previous result [18], which it supersedes. In addition, the shape of the photon energy spectrum is measured in the B meson rest frame. It is insensitive to NP [19] but can be used to determine the heavy quark expansion parameters m_b and μ_π^2 [20,21], related to the mass and momentum of the b quark within the B meson. These parameters are used to reduce the uncertainty in the extraction of the CKM elements $|V_{cb}|$ and $|V_{ub}|$ from semileptonic B meson decays [22–25].

This Letter summarizes a fully inclusive analysis of $B \to X_s\gamma$ decays collected from $e^+e^- \to \Upsilon(4S) \to B\bar{B}$ events. Full details are given in Ref. [26]. The photon from the decay of one B meson is measured, but X_s is not reconstructed. This avoids large uncertainties from the modeling of the X_s system, at the cost of large backgrounds, which need to be strongly suppressed. The principal backgrounds are from other $B\bar{B}$ decays containing a high-energy photon and from continuum $q\bar{q}$ ($q = udsc$) and $\tau^+\tau^-$ events. The continuum background, including a contribution from initial-state radiation, is suppressed principally by requiring a high-momentum charged lepton (''lepton tag'') from the nonsignal B decay, and also by discriminating against events with a more jetlike topology. The $B\bar{B}$ background to high-energy photons, dominated by π^0 and η decays, is reduced by vetoing reconstructed π^0 or η mesons. The residual continuum background is subtracted using off-resonance data collected at a center-of-mass (c.m.) energy 40 MeV below the $\Upsilon(4S)$, while the remaining $B\bar{B}$ background is estimated using a Monte Carlo (MC) simulation that has been corrected using data control samples. The photon energy spectrum is measured in the $\Upsilon(4S)$ rest frame. Quantities measured in this frame are denoted by an asterisk, e.g., E_γ^*.

The data were collected with the *BABAR* detector [27] at the PEP-II asymmetric-energy e^+e^- collider. The on-resonance integrated luminosity is 347.1 fb^{-1}, corresponding to $(382.8 \pm 4.2) \times 10^6$ $B\bar{B}$ events. Additionally, 36.4 fb^{-1} of off-resonance data are used. The *BABAR* MC simulation, based on GEANT4 [28], EVTGEN [29], and JETSET [30], is used to generate samples of B^+B^- and $B^0\bar{B}^0$ (excluding signal channels), $q\bar{q}$, $\tau^+\tau^-$, and signal events. The signal models used to compute efficiencies are based on QCD calculations in the ''kinetic scheme'' [20], ''shape function scheme'' [21], and in an earlier model [19]. These calculations approximate the X_s resonance structure with a smooth distribution in the hadronic mass m_{X_s}. The portion of the m_{X_s} spectrum below 1.1 GeV/c^2, where the $K^*(892)$ dominates, is replaced by a Breit-Wigner $K^*(892)$ distribution. The analysis is performed ''blind'' in the range $1.8 < E_\gamma^* < 2.9$ GeV; that is, the on-resonance data are not examined until all selection requirements are finalized and the corrected $B\bar{B}$ backgrounds determined. The signal range is limited by large $B\bar{B}$ backgrounds at low E_γ^*.

The event selection begins by requiring at least one photon candidate with $1.53 < E_\gamma^* < 3.50$ GeV. A photon candidate is an electromagnetic calorimeter (EMC) energy cluster with a lateral profile consistent with that of a single photon, isolated by 25 cm from any other cluster, and well contained in the calorimeter. Photons that are consistent with originating from an identifiable π^0 or $\eta \to \gamma\gamma$ decay are vetoed. Hadronic events are selected by requiring at least three reconstructed charged particles and the normalized second Fox-Wolfram moment R_2^* to be less than 0.9. To reduce radiative Bhabha and two-photon backgrounds, the number of charged particles plus half the number of photons with energy above 0.08 GeV is required to be at least 4.5.

About 20% of B mesons decay semileptonically to either e or μ. Leptons from these decays are emitted isotropically and tend to have higher momentum than the continuum background in which the lepton and photon candidates also tend to be anticollinear. To suppress the continuum background a tagging lepton ($\ell = e, \mu$) is required to have momentum $p_l^* > 1.05$ GeV/c and an angle relative to the photon $\cos\theta_{\gamma\ell}^* > -0.7$. The tag requirement does not compromise the inclusiveness of the $B \to X_s\gamma$ selection since the lepton comes from the recoiling B meson. The presence of a relatively high-energy neutrino in semileptonic B decays is used to further suppress the background by requiring the missing energy of the event to satisfy $E_{\rm miss}^* > 0.7$ GeV.

The sample is separated into electron and muon tags. For each, p_l^* and $\cos\theta_{\gamma\ell}^*$ are then combined in a neural network (NN) with eight event-shape variables that exploit the difference in topology between isotropic $B\bar{B}$ events and jetlike continuum events. The NN is trained to separate signal-like events from continuum background using MC samples. The $B\bar{B}$ background sample is excluded from the training because it is used for background subtraction and is topologically similar to the signal. The NN is validated with a $B \to X_s\pi^0$ data sample.

The selection criteria are optimized for statistical precision. This was done iteratively for five variables: the two NN outputs, the energies of the lower-energy photon in the π^0 and η vetoes, and $E_{\rm miss}^*$. The signal efficiency for the entire selection depends on E_γ^*, falling at lower values. This effect is significantly reduced from our previous analysis, lessening the uncertainty due to the assumed signal model (''model-dependence''). The efficiency integrated over the range $1.8 < E_\gamma^* < 2.8$ GeV is about 2.5%,

while only 0.0005% of the continuum and 0.013% of the $B\bar{B}$ background remain in the sample.

The remaining continuum background is estimated with off-resonance data scaled to the on-resonance luminosity and adjusted to account for the 40 MeV c.m. energy difference. The $B\bar{B}$ background is estimated with the $B\bar{B}$ MC sample. It consists predominantly of photons originating from π^0 or η decays ($\approx 80\%$ in the signal region), electrons ($\approx 10\%$) that are misreconstructed, not identified, or undergo hard bremsstrahlung, ω and η' decays ($\approx 4\%$), and $\bar{n}$'s ($\approx 2\%$) that fake photons by annihilating in the EMC. Each of the significant components is corrected by comparison with data control samples.

The π^0 and η background simulations are compared to data using the same selection criteria as for $B \to X_s\gamma$ but removing the π^0 and η vetos. For this comparison the high-energy photon requirement is relaxed to $E^*_\gamma > 1.03$ GeV to increase the size of the sample. The yields of π^0 and η are measured in bins of $E^*_{\pi^0(\eta)}$ by fitting the $\gamma\gamma$ mass distributions in on-resonance data, off-resonance data, and $B\bar{B}$ simulation. Correction factors to the π^0 and η components of the $B\bar{B}$ simulation are derived from these yields. An additional correction is applied to account for data-MC differences in the low-energy photon detection efficiency. This has an opposite effect on the control-sample π^0 and η selection than on the standard event selection, where finding a π^0 or η results in the event being vetoed.

As an antineutron control sample could not be isolated, this source of $B\overline{B}$ background is corrected by comparing simulation to data for inclusive antiproton yields in B decay and, using $\overline{\Lambda} \to \overline{p}\pi^+$ samples, for the EMC response to $\overline{p}$'s. The misreconstructed electron background is measured using $B \to XJ/\psi(e^+e^-)$ data. This sample closely models the particle multiplicity in $B \to X_s\gamma$ events. Bremsstrahlung in the detector is reliably simulated by GEANT4, so no correction is necessary. The small contributions from ω and η' decays are corrected in bins of E^*_γ using inclusive B decay data. Nearly all of the tagging leptons arise from $B \to X_c\ell\nu$. The yield of such events in the simulation is corrected as a function of lepton momentum according to previous *BABAR* measurements [31,32]. The complete $B\bar{B}$ background estimation incorporates the correction factors and uncertainties and includes correlations between E^*_γ bins. The dominant uncertainties originate from the π^0, η, and misreconstructed electron corrections.

Figure 1 shows the measured E^*_γ spectrum after subtracting both continuum and $B\bar{B}$ backgrounds. The systematic errors are due to the $B\bar{B}$ subtraction uncertainty. The region $1.53 < E^*_\gamma < 1.80$ GeV is dominated by $B\bar{B}$ background, while the higher-energy range $2.9 < E^*_\gamma < 3.5$ GeV contains only continuum background. These regions are used to validate the background subtraction procedure. In the higher-energy range there are -100 ± 138(stat) events.

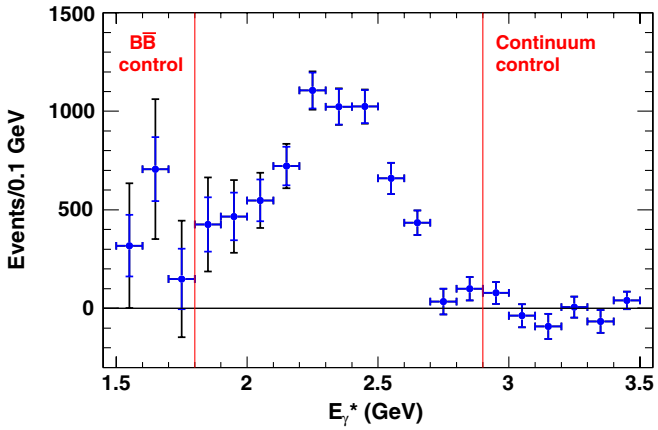

FIG. 1 (color online). The measured E^*_γ photon energy spectrum after background subtraction, uncorrected for efficiency and resolution smearing. The inner error bars are statistical only, while the outer include systematic errors added in quadrature.

In the lower-energy region there are 1252 ± 272(stat) $\pm$ 841(syst) events. Allowing for an average of 275 signal events from a range of plausible signal models, and for correlations between the bins, the latter result is consistent with zero to within 1 standard deviation (1σ).

To extract BFs and the shape of the spectrum, it is necessary to first correct for efficiency. Theoretical predictions are made for the true E_γ in the B meson rest frame, whereas the E^*_γ is measured in the $\Upsilon(4S)$ frame. Hence it is also necessary to correct for the asymmetric EMC resolution and the Doppler smearing due to the motion of the B meson in the $\Upsilon(4S)$ rest frame. The efficiency and smearing corrections depend upon the assumed signal shape due to the effects of bin migration. In both the kinetic and shape function schemes, this shape is parametrized by m_b and μ^2_π. The Heavy Flavor Averaging Group (HFAG) [33] has extracted values and uncertainties in the kinetic scheme by fitting moments of inclusive distributions in $B \to X_c\ell\nu$ decays and previous $B \to X_s\gamma$ measurements, and has also translated them to the shape function scheme. These results define the nominal signal model (kinetic scheme) used for the BF measurement, along with a model-dependence uncertainty (kinetic and shape function schemes). To provide an independent measurement of the shape of the spectrum, the measured spectrum is unfolded using an iterative technique that reduces sensitivity to the signal model. In this case the initial signal model and model-dependence uncertainty are based on the data rather than the HFAG parameters. The effects of efficiency and smearing cancel in the A_{CP} measurement so it is extracted directly from the measured E^*_γ yield separated by lepton tag charge.

The BF is computed from

$$\mathcal{B}(B \to X_{s+d}\gamma) = \alpha \mathrm{S}/(2N_{B\bar{B}}\epsilon_{\mathrm{sig}}),$$

where S is the signal yield integrated over the E^*_γ ranges 1.8, 1.9, 2.0 to 2.8 GeV, ϵ_{sig} is the signal efficiency, and

TABLE I. The measured BF, first, and second moments (± stat ± syst ± model) for different ranges of E_γ in the B rest frame. Correlations between the energy ranges are given in Ref. [26].

E_γ Range (GeV)	$\mathcal{B}(B \to X_s\gamma)$ (10^{-4})	$\langle E_\gamma \rangle$ (GeV)	$\langle (E_\gamma - \langle E_\gamma \rangle)^2 \rangle$ (GeV^2)
1.8 to 2.8	$3.21 \pm 0.15 \pm 0.29 \pm 0.08$	$2.267 \pm 0.019 \pm 0.032 \pm 0.003$	$0.0484 \pm 0.0053 \pm 0.0077 \pm 0.0005$
1.9 to 2.8	$3.00 \pm 0.14 \pm 0.19 \pm 0.06$	$2.304 \pm 0.014 \pm 0.017 \pm 0.004$	$0.0362 \pm 0.0033 \pm 0.0033 \pm 0.0005$
2.0 to 2.8	$2.80 \pm 0.12 \pm 0.14 \pm 0.04$	$2.342 \pm 0.010 \pm 0.008 \pm 0.005$	$0.0251 \pm 0.0021 \pm 0.0013 \pm 0.0009$

$N_{B\bar{B}}$ is the number of $B\bar{B}$ pairs in the sample. The factor α, which is close to unity, corrects for resolution and Doppler smearing and is computed with the nominal signal model. The model-dependence errors on the BF associated with the efficiency and the smearing correction are fully correlated. The results for the three energy ranges are given in Table I. The BFs have been corrected by a factor $1/(1 + (|V_{td}|/|V_{ts}|)^2) = 0.958 \pm 0.003$ [34] to remove the contribution from $b \to d\gamma$. The most significant systematic error is from the corrections to the $B\bar{B}$ background simulation, which in the range 1.8 GeV $< E_\gamma <$ 2.8 GeV contributes 7.8% to a total systematic uncertainty of 9.0%. Additional contributions added in quadrature, all energy-independent, arise from uncertainties in the selection efficiency (3.1%), predominantly due to the high-energy photon and NN selections, the semileptonic BF for B meson decays, and the modeling of the X_s system. Correlations between the $B\bar{B}$ and the signal efficiency systematic errors contribute an additional 2.9% uncertainty. Finally, there is a 1.1% uncertainty in $N_{B\bar{B}}$.

To obtain an E_γ spectrum in the B rest frame, the E_γ^* spectrum shown in Fig. 1 is corrected for selection efficiency, and the resolution smearing and Doppler smearing are unfolded. A simplified version [35] of an iterative unfolding technique [36] is used. The method starts with an initial signal model that, when passed through the detector simulation and event selection, closely resembles the data (shape function scheme with $m_b = 4.51$ GeV, $\mu_\pi^2 = 0.46$ GeV^2). This model is used to correct for efficiency and unfold the data. A fraction, determined by a bin-dependent regularization function, of the difference between the unfolded data and the initial signal model is used to adjust the signal model, and the process is iterated until it converges. Only one iteration is necessary. The results are shown in Fig. 2. This technique preserves fluctuations in the spectrum and reduces the model error. The model-dependence uncertainty is computed using an initial model that is approximately 1σ lower than the data in Fig. 1 in the region with significant $B\bar{B}$ background ($1.8 < E_\gamma^* < 2.1$ GeV). The error is the absolute value of the difference bin by bin after unfolding. It is small except near the kinematic limit, $E_\gamma \approx m_B/2$, where the sharply falling edge leads to strongly anticorrelated differences in adjacent bins. To reduce this effect, the 100-MeV bins between 2.4 and 2.8 GeV are combined into 200-MeV bins. The spectral shape and the full covariance matrix, provided in Ref. [26], are used to compute the first and second moments in Table I. They can also be used to fit any theoretical prediction for the spectral shape. The BFs computed from the sum of the $\Delta\mathcal{B}$ in Fig. 2 are consistent with the values given in Table I [26].

Finally the E_γ^* sample is divided into B and $\bar{B}$ decays, using the charge of the lepton tag, to measure $A_{CP}^{\rm meas}(B \to X_{s+d}\gamma) = (N^+ - N^-)/(N^+ + N^-)$, where $N^{+(-)}$ are the positively (negatively) tagged signal yields. A_{CP} is then given by $A_{CP} = A_{CP}^{\rm meas}/(1 - 2\omega)$, where ω is the mistag fraction. To maximize the statistical precision a requirement of $2.1 < E_\gamma^* < 2.8$ GeV is made. This is determined from simulation and does not bias the SM prediction for the asymmetry [37]. The yields are $N^+ = 2620 \pm 158$(stat) and $N^- = 2389 \pm 151$(stat). The bias on A_{CP} due to charge asymmetry in the detector response or $B\bar{B}$ background is measured to be $\Delta A_{CP}^{\rm meas}(B \to X_{s+d}\gamma) = -0.004 \pm 0.013$, using events in the $B\bar{B}$ control region to check for a background asymmetry, and using several event samples ($e^+e^- \to e^+e^-\gamma$, $e^+e^- \to \mu\mu\gamma$, and $B \to K^{(*)}J/\psi(\ell^+\ell^-)$) to check for a lepton tag asymmetry. The mistag fraction $\omega = 0.133 \pm 0.006$ is dominated by $B^0\bar{B}^0$ mixing, which contributes 0.093 ± 0.001 [34], with

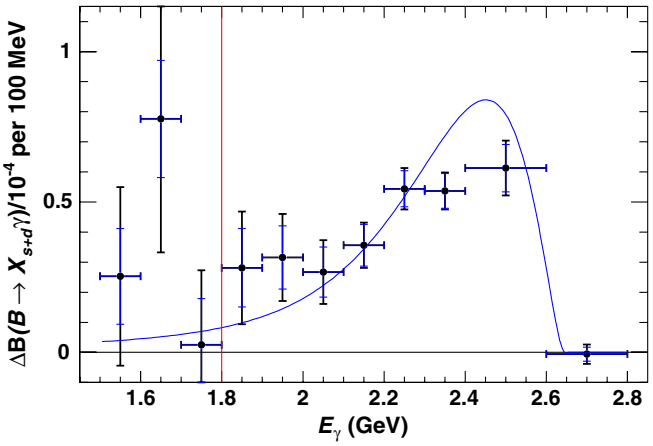

FIG. 2 (color online). The E_γ photon energy spectrum corrected for efficiency, resolution, and Doppler smearing, shown as a partial branching fraction $\Delta\mathcal{B}$. The inner error bars are statistical and the outer include systematic errors added in quadrature. The vertical line shows the boundary between the lower control region and the signal region. The curve is the kinetic scheme model using HFAG world average parameters, normalized to data in the range $1.8 < E_\gamma^B < 2.8$ GeV.

an additional 0.040 ± 0.005 arising from wrong-sign leptons from the B decay chain and from misidentifcation of hadrons as leptons. After correcting for charge bias and mistagging it is found

$$A_{CP} = 0.057 \pm 0.060(\text{stat}) \pm 0.018(\text{syst}).$$

The systematic error includes relative uncertainties from the $B\bar{B}$ background subtraction (2.2%) and mistagging (1.8%). The uncertainty due to differences in the $B \to X_s\gamma$ and $B \to X_d\gamma$ spectra is negligible.

In summary, the photon spectrum of $B \to X_{s+d}\gamma$ decays has been measured and used to extract the branching fraction, spectral moments, and A_{CP}. Previous inclusive measurements of $B \to X_s\gamma$ have been presented by the CLEO [38], *BABAR* [18], and Belle [39] Collaborations. The measured branching fraction $\mathcal{B}(B \to X_s\gamma) = (3.21 \pm 0.15 \pm 0.29 \pm 0.08) \times 10^{-4}$ ($1.8 < E_\gamma < 2.8$ GeV) is comparable in precision to the Belle result, $(3.36 \pm 0.13 \pm 0.25 \pm 0.01) \times 10^{-4}$, but with a data set that has 60% smaller integrated luminosity. The BF for $1.8 < E_\gamma < 2.8$ GeV is extrapolated to the range $E_\gamma > 1.6$ GeV using a factor of $1/(0.968 \pm 0.006)$ determined by HFAG. This results in $\mathcal{B}(B \to X_s\gamma) = (3.31 \pm 0.16 \pm 0.30 \pm 0.09) \times 10^{-4}$ for $E_\gamma > 1.6$ GeV, in good agreement with the SM prediction. The extrapolated $\mathcal{B}(B \to X_s\gamma)$ can be used to constrain NP. For example, in a type-II two-Higgs-doublet model [10,40] the region $M_{H^\pm} < 327$ GeV is excluded independent of $\tan\beta$ at 95% confidence level. This limit is far more stringent than that from direct searches at the LHC [41,42]. The A_{CP} measurement is the most precise to date and can be used to constrain nonminimal flavor-violating models [11]. The measured moments and spectra provide input to improve the precision on the HFAG estimation of m_b and μ_π^2, which will result in a reduced error on $|V_{ub}|$. Finally, the improved technique presented in this Letter can be applied with increased precision at future Super B factories.

We are grateful for the excellent luminosity and machine conditions provided by our PEP-II colleagues, and for the substantial dedicated effort from the computing organizations that support *BABAR*. The collaborating institutions wish to thank SLAC for its support and kind hospitality. This work is supported by DOE and NSF (USA), NSERC (Canada), CEA and CNRS-IN2P3 (France), BMBF and DFG (Germany), INFN (Italy), FOM (The Netherlands), NFR (Norway), MES (Russia), MICIIN (Spain), and STFC (United Kingdom). Individuals have received support from the Marie Curie EIF (European Union) and the A. P. Sloan Foundation (USA).

*Deceased.
†Now at the University of Tabuk, Tabuk 71491, Saudi Arabia.
‡Also with Università di Perugia, Dipartimento di Fisica, Perugia, Italy.
§Now at the University of Huddersfield, Huddersfield HD1 3DH, United Kingdom.
‖Now at University of South Alabama, Mobile, AL 36688, USA.
¶Also with Università di Sassari, Sassari, Italy.

[1] S. Bertolini, F. Borzumati, and A. Masiero, Nucl. Phys. **B294**, 321 (1987).
[2] J. L. Hewett and J. D. Wells, Phys. Rev. D **55**, 5549 (1997).
[3] M. S. Carena, D. Garcia, U. Nierste, and C. E. M. Wagner, Phys. Lett. B **499**, 141 (2001).
[4] H. Baer and C. Balazs, J. Cosmol. Astropart. Phys. 05 (2003) 006.
[5] W. Huo and S. Zhu, Phys. Rev. D **68**, 097301 (2003).
[6] A. J. Buras, P. H. Chankowski, J. Rosiek, and L. Slawianowska, Nucl. Phys. **B659**, 3 (2003).
[7] M. Frank and S. Nie, Phys. Rev. D **65**, 114006 (2002).
[8] K. Agashe, N. G. Deshpande, and G. H. Wu, Phys. Lett. B **514**, 309 (2001).
[9] I. I. Y. Bigi, N. G. Uraltsev, and A. I. Vainshtein, Phys. Lett. B **293**, 430 (1992).
[10] M. Misiak *et al.*, Phys. Rev. Lett. **98**, 022002 (2007).
[11] T. Hurth, E. Lunghi, and W. Porod, Nucl. Phys. **B704**, 56 (2005).
[12] J. M. Soares, Nucl. Phys. **B367**, 575 (1991).
[13] T. Hurth and T. Mannel, Phys. Lett. B **511**, 196 (2001).
[14] M. Benzke, S. J. Lee, M. Neubert, and G. Paz, Phys. Rev. Lett. **106**, 141801 (2011).
[15] T. E. Browder, T. Gershon, D. Pirjol, A. Soni, and J. Zupan, Rev. Mod. Phys. **81**, 1887 (2009).
[16] B. O'Leary *et al.* (SuperB Collaboration), arXiv:1008.1541.
[17] T. Aushev *et al.*, arXiv:1002.5012.
[18] B. Aubert *et al.* (*BABAR* Collaboration), Phys. Rev. Lett. **97**, 171803 (2006).
[19] A. L. Kagan and M. Neubert, Eur. Phys. J. C **7**, 5 (1999).
[20] D. Benson, I. I. Bigi, and N. Uraltsev, Nucl. Phys. **B710**, 371 (2005).
[21] M. Neubert, Phys. Rev. D **72**, 074025 (2005).
[22] C. W. Bauer, Z. Ligeti, M. Luke, A. V. Manohar, and M. Trott, Phys. Rev. D **70**, 094017 (2004).
[23] B. O. Lange, M. Neubert, and G. Paz, Phys. Rev. D **72**, 073006 (2005).
[24] C. W. Bauer, Z. Ligeti, M. Luke, and A. V. Manohar, Phys. Rev. D **67**, 054012 (2003).
[25] P. Gambino, P. Giordano, G. Ossola, and N. Uraltsev, J. High Energy Phys. 10 (2007) 058.
[26] J. Lees *et al.* (*BABAR* Collaboration), arXiv:1207.2690 [Phys. Rev. D (to be published)].
[27] B. Aubert *et al.* (*BABAR* Collaboration), Nucl. Instrum. Methods Phys. Res., Sect. A **479**, 1 (2002).
[28] S. Agostinelli *et al.* (GEANT4 Collaboration), Nucl. Instrum. Methods Phys. Res., Sect. A **506**, 250 (2003).
[29] D. J. Lange, Nucl. Instrum. Methods Phys. Res., Sect. A **462**, 152 (2001).
[30] T. Sjöstrand, Comput. Phys. Commun. **82**, 74 (1994).
[31] B. Aubert *et al.* (*BABAR* Collaboration), Phys. Rev. D **69**, 111104 (2004).
[32] B. Aubert *et al.* (*BABAR* Collaboration), Phys. Rev. D **81**, 032003 (2010).

[33] D. Asner *et al.* (HFAG Collaboration), arXiv:1010.1589v3.
[34] K. Nakamura *et al.* (Particle Data Group), J. Phys. G **37**, 075021 (2010), and 2011 partial update for the 2012 edition.
[35] B. Aubert *et al.* (*BABAR* Collaboration), Phys. Rev. Lett. **103**, 231801 (2009).
[36] B. Malaescu, arXiv:0907.3791v1.
[37] A. L. Kagan and M. Neubert, Phys. Rev. D **58**, 094012 (1998).
[38] S. Chen *et al.* (CLEO Collaboration), Phys. Rev. Lett. **87**, 251807 (2001).
[39] A. Limosani *et al.* (Belle Collaboration), Phys. Rev. Lett. **103**, 241801 (2009).
[40] U. Haisch, arXiv:0805.2141v2.
[41] S. Chatrchyan *et al.* (CMS Collaboration), J. High Energy Phys. 07 (2012) 143.
[42] G. Aad *et al.* (ATLAS Collaboration), J. High Energy Phys. 06 (2012) 039.